Surface-roughness effect on capacitance and leakage current of an insulating film

Y.-P. Zhao, G.-C. Wang, and T.-M. Lu
Department of Physics, Applied Physics, and Astronomy, and Center for Integrated Electronics and Electronics Manufacturing, Rensselaer Polytechnic Institute, Troy, New York 12180-3590

G. Palasantzas and J. Th. M. De Hosson
Department of Applied Physics, Materials Science Center, University of Groningen, Nijenborgh 4, 9747 AG Groningen, The Netherlands
(Received 9 April 1999)

Effects of surface roughness on electrical properties of a thin insulating film capacitor with one smooth electrode plate and one rough electrode plate are investigated. The electrode plate roughness is described in terms of self-affine fractal scaling through the roughness exponent α, the root-mean square (rms) roughness amplitude w, and the correlation length ξ. The electric field, capacitance, and leakage current show similar qualitative changes with the roughness parameters: they all increase as w increases, and also increase as either ξ or α decreases. [S0163-1829(99)10035-3]

I. INTRODUCTION

The rough morphology of surfaces and interfaces and the presence of material defects (e.g., dislocations, impurities, etc.) can alter the operational conditions of microelectronic devices.[1,2] An enormous amount of effort is underway in order to understand the electronic and electrical properties of devices affected by these imperfections which prevent potential device applications. Examples are storage capacitors for dynamic and static random access memories (CDRAM and SRAM), alternating current thin-film electroluminescent devices, etc.[3–5] Indeed, many proposed device geometries require the growth of high-quality films. However, kinetic effects can induce roughness and defects formation in films depending on the material, the substrate on which the growth commences, and the deposition conditions.

Examples of roughness effects on electrical properties of devices include, but are not limited to, the following important cases. Random rough surfaces have been shown to influence drastically the image potential of a charge situated in the vicinity of a plane interface between a vacuum and a dielectric.[6] Such roughness effects could have a strong influence on an inversion layer at a semiconductor/oxide interface, since it can cause shifts of electronic energy levels[6] and thus alter the device function. Surface/interface roughness has been shown to influence strongly the electrical conductivity of semiconducting and metallic thin films.[7] The presence of a rough metal/insulator interface (e.g., for polycrystalline and multilayer $BaTiO_3$ thin films) has been shown to influence the field breakdown mechanism.[4]

Thin insulating films have been used as a gate oxide and dielectric interlayer (SiO_2),[1,8,9] DRAM capacitor ($Ba_{1-x}Sr_xTiO_3$),[10,11] and a decoupling capacitor (Ta_2O_5) (Ref. 12) in high-performance packaging. A large number of experiments have found that the surface/interface morphology has a great influence on the electrical properties of those dielectrics, especially the leakage current. For examples, Chin *et al.* showed that the presence of native oxide will increase the interface roughness, gate oxide leakage current, and stress-induced hole traps.[8] Li *et al.* also found that with increasing surface roughness, the leakage currents of BST ($Ba_{1-x}Sr_xTiO_3$), SBT ($SrBi_2Ta_2O_9$) and PZT ($PbZr_{1-x}Ti_xO_3$) increase.[11] Chen *et al.* demonstrated that the roughness of the polyimide substrate has a strong influence on the electrical properties and yields of thin TaO_x capacitors.[12] Both the leakage current and the breakdown field strength increase with increasing substrate roughness. Furthermore, they demonstrated that using benzocyclobitene (BCB) to planarize the substrate can greatly improve the capacitor yield and performance.[12] All these experimental results show a qualitative trend: the leakage current increases with the increase of surface roughness.

For a parallel-plate capacitor, the capacitance C_0 depends on dielectric film thickness h_0 as $C_0 \sim 1/h_0$. A change of h_0 allows a change in C_0. However, defects such as pinholes in the dielectric film[13] and roughness at the metal/dielectric interface[3] can alter electric-field characteristics within the capacitor area, effectively influencing the dielectric strength of the insulating material. Another important issue is the accuracy in using the capacitance measurement to determine the dielectric constant of a thin insulating film. This is a standard technique for microelectronics manufacturing. Now there are growing interests on finding suitable low dielectric constant (low-k) material to substitute the SiO_2 in order to reduce the resistor-capacitor (RC) delay. However, as we will see later, the roughness will cause an overestimation of the dielectric constant of a material, or introduce a large error bar in the measurement.

Up to now a quantitative study of metal/dielectric interface roughness effects on the electric field, capacitance, and leakage current within a thin-film capacitor is still missing. In this paper we will address the above issues using a simple parallel-plate capacitor with one rough electrode. We combine simple roughness models that describe self-affine random rough surfaces and a perturbation solution of the Poisson equation for a thin-film capacitor.

II. ELECTRIC POTENTIAL AND ELECTRIC FIELD OF A CAPACITOR WITH A SINGLE ROUGH BOUNDARY

Consider a parallel-plate capacitor with only one rough electrode surface at potential V and the other one (substrate)

 ©1999 The American Physical Society

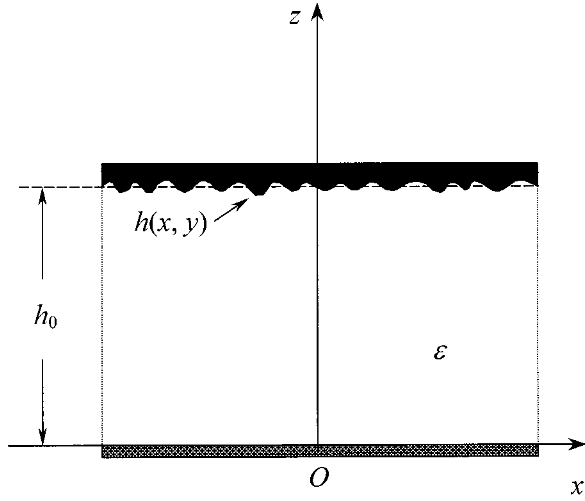

FIG. 1. Schematic of a parallel plate capacitor with a rough boundary. ε is the dielectric constant of the filling material, h_0 is the average thickness of the dielectrics, and $h(x,y)$ is the fluctuation of the thickness. $\boldsymbol{\rho}=(x,y)$ is the in-plane position.

is smooth at potential zero, as shown in Fig. 1. Here ε is the dielectric constant of the filling material, h_0 is the average thickness, and $h(x,y)$ is the surface height fluctuation. In order to calculate the electrostatic potential, one needs to solve the Laplace equation between the capacitor planes,

$$\nabla^2\Phi(x,y,z)=0, \tag{1}$$

that obeys the boundary conditions

$$\Phi(x,y,z=0)=0, \tag{2}$$

and

$$\Phi[x,y,z=f(x,y)]=V. \tag{3}$$

Here Φ is the electrostatic potential, and $z=f(x,y)$ is the rough electrode surface. If we assume that $f(x,y)=h_0+\lambda h(x,y)$, where $\lambda\ll 1$, then we can apply a perturbation method for the potential on the rough boundary to solve the Laplace equation, [Eq. (1)]. Thus the boundary condition [Eq. (3)] can be expanded as a Taylor series in the form

$$\Phi(x,y,h_0)+\Phi_z(x,y,h_0)\lambda h(x,y)+\frac{1}{2!}\Phi_{zz}(x,y,h_0)\lambda^2h^2(x,y)+\cdots=V, \tag{4}$$

where $\Phi_z=\partial\Phi/\partial z$, $\Phi_{zz}=\partial^2\Phi/\partial z^2$, and so on. We also assume that the potential takes a similar perturbative form

$$\Phi(x,y,z)=\Phi^{(0)}(x,y,z)+\lambda\Phi^{(1)}(x,y,z)+\lambda^2\Phi^{(2)}(x,y,z)+\cdots. \tag{5}$$

Substituting Eq. (5) into Eq. (1), we find that, for any order of perturbation, $\Phi^{(n)}(x,y,z)$ satisfies the Laplace equation

$$\nabla^2\Phi^{(n)}(x,y,z)=0. \tag{6}$$

Furthermore, the boundary conditions for various orders of perturbation are as follows: For the zeroth order,

$$\Phi^{(0)}(x,y,z=0)=0, \tag{7a}$$

$$\Phi^{(0)}(x,y,z=h_0)=V, \tag{7b}$$

which yields the solution

$$\Phi^{(0)}(x,y,z)=\frac{Vz}{h_0}. \tag{8}$$

For the first order,

$$\Phi^{(1)}(x,y,z=0)=0, \tag{9a}$$

$$\Phi^{(1)}(x,y,z=h_0)=-h(x,y)\Phi_z^{(0)}(x,y,h_0). \tag{9b}$$

For the second order,

$$\Phi^{(2)}(x,y,z=0)=0, \tag{10a}$$

$$\Phi^{(2)}(x,y,z=h_0)=-h(x,y)\Phi_z^{(1)}(x,y,h_0)-\tfrac{1}{2}h^2(x,y)\Phi_{zz}^{(0)}(x,y,h_0). \tag{10b}$$

For a perturbation higher than the first order, we can employ the Fourier transform technique to solve the Laplace equation with boundary conditions similar to Eqs. (9) and (10):

$$\nabla^2\Phi^{(n)}(x,y,z)=\frac{\partial^2}{\partial z^2}\Phi^{(n)}(x,y,z)+\nabla_\rho^2\Phi^{(n)}(x,y,z)=0, \tag{11}$$

where $\boldsymbol{\rho}=(x,y)$ represents the position vector in the x-y plane. Performing a Fourier transform in the x-y plane according to the equations

$$\tilde{\Phi}^{(n)}(\mathbf{k},z)=\frac{1}{(2\pi)^2}\int d\boldsymbol{\rho}\,\Phi^{(n)}(\boldsymbol{\rho},z)e^{i\mathbf{k}\cdot\boldsymbol{\rho}}, \tag{12}$$

$$\Phi^{(n)}(\boldsymbol{\rho},z)=\int d\mathbf{k}\,\tilde{\Phi}^{(n)}(\mathbf{k},z)e^{-i\mathbf{k}\cdot\boldsymbol{\rho}}, \tag{13}$$

then the Laplacian equation takes the form

$$\frac{\partial^2}{\partial z^2}\tilde{\Phi}^{(n)}(\mathbf{k},z)-k^2\tilde{\Phi}^{(n)}(\mathbf{k},z)=0. \tag{14}$$

The general solution of Eq. (14) can be put in a form

$$\tilde{\Phi}^{(n)}(\mathbf{k},z)=A^{(n)}(\mathbf{k})e^{kz}+B^{(n)}(\mathbf{k})e^{-kz}. \tag{15}$$

Applying the boundary condition at $z=0$, one has

$$A^{(n)}(\mathbf{k})=-B^{(n)}(\mathbf{k}), \tag{16}$$

which alternatively implies that

$$\tilde{\Phi}^{(n)}(\mathbf{k},z)=2A^{(n)}(\mathbf{k})\sinh(kz). \tag{17}$$

$A^{(n)}(\mathbf{k})$ can be determined by the boundary condition at $z=h_0$. For the first-order perturbation we obtain potentials in Fourier and real spaces, respectively:

$$\tilde{\Phi}^{(1)}(\mathbf{k},z)=-\frac{V}{h_0}\frac{\sinh(kz)}{\sinh(kh_0)}\tilde{h}(\mathbf{k}), \tag{18}$$

$$\Phi^{(1)}(\boldsymbol{\rho},z)=-\frac{V}{h_0}\int d\mathbf{k}\frac{\sinh(kz)}{\sinh(kh_0)}\tilde{h}(\mathbf{k})e^{-i\mathbf{k}\cdot\boldsymbol{\rho}}. \tag{19}$$

Similarly, by using the property of convolution for Fourier transform for the second-order perturbation, we obtain

$$\tilde{\Phi}^{(2)}(\mathbf{k},z)=\frac{V}{h_0}\int d\mathbf{k}'\frac{\cosh(k'h_0)\sinh(kz)}{\sinh(k'h_0)\sinh(kh_0)}\times k'\tilde{h}(\mathbf{k}')\tilde{h}(\mathbf{k}-\mathbf{k}'), \tag{20}$$

$$\Phi^{(2)}(\boldsymbol{\rho},z)=\frac{V}{h_0}\int d\mathbf{k}\int d\mathbf{k}'\frac{\cosh(k'h_0)\sinh(kz)}{\sinh(k'h_0)\sinh(kh_0)}\times k'\tilde{h}(\mathbf{k}')\tilde{h}(\mathbf{k}-\mathbf{k}')e^{-i\mathbf{k}\cdot\boldsymbol{\rho}}. \tag{21}$$

If we set $\lambda=1$, then the electrostatic potential between two plates (electrodes) can be approximated by

$$\Phi\approx\Phi^{(0)}+\Phi^{(1)}+\Phi^{(2)}=\frac{Vz}{h_0}-\frac{V}{h_0}\int d\mathbf{k}\frac{\sinh(kz)}{\sinh(kh_0)}\tilde{h}(\mathbf{k})e^{-i\mathbf{k}\cdot\boldsymbol{\rho}}+\frac{V}{h_0}\int d\mathbf{k}\int d\mathbf{k}'\frac{\cosh(k'h_0)\sinh(kz)}{\sinh(k'h_0)\sinh(kh_0)}k'\tilde{h}(\mathbf{k}')\times\tilde{h}(\mathbf{k}-\mathbf{k}')e^{-i\mathbf{k}\cdot\boldsymbol{\rho}}. \tag{22}$$

Furthermore, the electric field E can be calculated as

$$\begin{aligned}E(x,y,z)&=-\nabla\Phi=-\nabla\Phi^{(0)}-\nabla\Phi^{(1)}-\nabla\Phi^{(2)}-\cdots\\&=-\frac{V}{h_0}\hat{\mathbf{e}}_3+\frac{V}{h_0}\int d\mathbf{k}\frac{\cosh(kz)}{\sinh(kh_0)}k\tilde{h}(\mathbf{k})e^{-i\mathbf{k}\cdot\boldsymbol{\rho}}\hat{\mathbf{e}}_3\\&\quad-\frac{V}{h_0}\int d\mathbf{k}\int d\mathbf{k}'\frac{\cosh(k'h_0)\cosh(kz)}{\sinh(k'h_0)\sinh(kh_0)}k'k\tilde{h}(\mathbf{k}')\times\tilde{h}(\mathbf{k}-\mathbf{k}')e^{-i\mathbf{k}\cdot\boldsymbol{\rho}}\hat{\mathbf{e}}_3\\&\quad-\frac{V}{h_0}\int d\mathbf{k}\frac{\sinh(kz)}{\sinh(kh_0)}k\tilde{h}(\mathbf{k})e^{-i\mathbf{k}\cdot\boldsymbol{\rho}}i\mathbf{k}\\&\quad+\frac{V}{h_0}\int d\mathbf{k}\int d\mathbf{k}'\frac{\cosh(k'h_0)\sinh(kz)}{\sinh(k'h_0)\sinh(kh_0)}k'\tilde{h}(\mathbf{k}')\times\tilde{h}(\mathbf{k}-\mathbf{k}')e^{-i\mathbf{k}\cdot\boldsymbol{\rho}}i\mathbf{k}+\cdots,\end{aligned} \tag{23}$$

where $\hat{\mathbf{e}}_3$ is the unit vector in the z direction.

III. SELF-AFFINE ROUGHNESS SPECTRUM

A wide variety of surface/interface roughness occurring in nature is well described by self-affine fractal scaling.[14] Examples include the nanometer scale topology of vapor-deposited metal films, eroded and fractured surfaces, etc. For self-affine fractals the roughness spectrum $\langle|\tilde{h}(\mathbf{k})|^2\rangle$ scales as[14]

$$\langle|\tilde{h}(\mathbf{k})|^2\rangle\propto\begin{cases}k^{-2-2\alpha} & \text{if } k\xi\gg1\\ \text{const} & \text{if } k\xi\ll1\end{cases}, \tag{24}$$

with the roughness exponent α being a measure of the degree of surface irregularity, and ξ the lateral correlation length.[15] Small values of α characterize more jagged or irregular surfaces at short roughness wavelengths ($<\xi$). The scaling behavior depicted by Eq. (24) can be described by a simple Lorentzian model,[16]

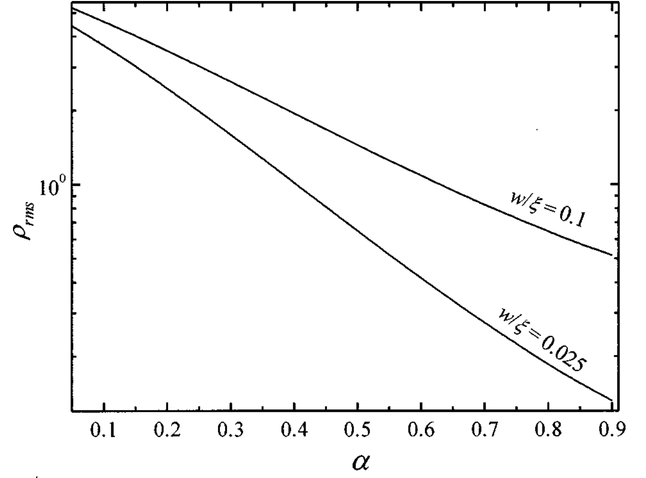

FIG. 2. Semilog plot of the rms local surface slope $\rho_{\mathrm{rms}}=\langle|\nabla h|^2\rangle^{1/2}$ as a function of roughness exponent α for two very different roughness parameter ratios w/ξ ($a_0=0.3$ nm, $w=2.0$ nm, and $\xi=20$ and 80 nm).

$$\langle|\tilde{h}(\mathbf{k})|^2\rangle=\frac{A}{(2\pi)^5}\frac{w^2\xi^2}{(1+ak^2\xi^2)^{1+\alpha}}, \tag{25}$$

with $a=(1/2\alpha)[1-(1+ak_c^2\xi^2)^{-\alpha}]$ if $0<\alpha<1$, and $a=(1/2)\ln[1+ak_c^2\xi^2]$ if $\alpha=0$. Here A is the area of the flat electrode plate we considered, and k_c is the upper cutoff of the spatial frequency. Other roughness models, which satisfy the scaling relation, depicted by Eq. (24), can be found in Refs. 14, 15, and 17.

IV. ROUGHNESS EFFECTS ON ELECTRICAL POTENTIAL AND ELECTRIC FIELD IN A CAPACITOR WITH ONE ROUGH ELECTRODE

Our calculations have been performed in the limit of weak roughness ($|\nabla h|<1$) or alternatively small rms local surface slopes $\rho_{\mathrm{rms}}=\langle|\nabla h|^2\rangle^{1/2}<\mathbf{k};11$, and small rms roughness amplitudes w such that $w\ll h_0$. For random self-affine rough surfaces, ρ_{rms} has been shown to scale as $\rho_{\mathrm{rms}}\propto w/\xi^{\alpha}$.[18,19] Figure 2 is a plot of this relation and shows that the rms local slope ρ_{rms} strongly depends on the roughness exponent α. The value of ρ_{rms} decreases by more than one order of magnitude as α increases from 0 to 1, even for small roughness parameter ratios w/ξ.

In the following we will assume statistically stationary surfaces up to the second order (translation invariant) or

$$\langle\tilde{h}(\mathbf{k})\tilde{h}(\mathbf{k}')\rangle=\frac{(2\pi)^4}{A}\langle|\tilde{h}(\mathbf{k})|^2\rangle\delta(\mathbf{k}+\mathbf{k}'), \tag{26}$$

Performing an ensemble average of Eq. (22) (taking into account that $\langle\tilde{h}(\mathbf{k})\rangle=0$) and substituting Eq. (26) into Eq. (22), one obtains the dominant terms in the electrostatic potential:

$$\langle\Phi\rangle=\Phi^{(0)}+\langle\Phi^{(2)}\rangle, \tag{27}$$

$$\Phi^{(0)} = \frac{Vz}{h_0},$$

$$\langle \Phi^{(2)} \rangle = (2\pi)^4 \frac{Vz}{Ah_0^2} \int_{0<k<k_c} \frac{\cosh(k' h_0)}{\sinh(k' h_0)} \times k' \langle |\tilde{h}(\mathbf{k}')|^2 \rangle d\mathbf{k}'. \quad (28)$$

Equation (28) shows that surface roughness causes an additional potential $\langle \Phi^{(2)} \rangle$ across the film, and this additional potential is still proportional to the distance z from the bottom plate. Therefore, the effect of roughness increases the effective potential $\langle \Phi \rangle$ between the two plates. As a result, the average electric field increases (where the average transverse fields are zero)

$$\langle \mathbf{E} \rangle = \mathbf{E}^{(0)} + \langle \mathbf{E}_z^{(2)} \rangle, \quad (29)$$

$$\mathbf{E}^{(0)} = -\frac{V}{h_0} \hat{\mathbf{e}}_3,$$

$$\langle \mathbf{E}_z^{(2)} \rangle = -(2\pi)^4 \frac{V}{Ah_0^2} \int_{0<k<k_c} \frac{\cosh(k' h_0)}{\sinh(k' h_0)} \times k' \langle |\tilde{h}(\mathbf{k}')|^2 \rangle d\mathbf{k}' \hat{\mathbf{e}}_3, \quad (30)$$

i.e., the roughness increases the average electric field inside the insulating film, or in other words, the effective thickness of the insulating film decreases. Substituting Eq. (25) into Eq. (30), and normalizing w, ξ and k' by h_0 as $\Delta = w/h_0$, $L = \xi/h_0$, and $q = kh_0$, respectively, Eq. (29) becomes

$$\frac{\langle E \rangle}{E^{(0)}} = 1 + \Delta^2 L^2 \int_0^{q_c} \frac{q^2 \coth(q)}{(1 + aL^2 q^2)^{1+\alpha}} dq. \quad (31)$$

Equation (31) clearly shows that roughness increases the average electric field in the film. The increased field $\langle \Delta E \rangle = \langle E \rangle - E^{(0)}$ is proportional to the square of interface width w, and also has a complicated relationship with both the lateral correlation length ξ and the roughness exponent α. Figure 3 shows the dependence of the electric field ratio $\langle E \rangle / E^{(0)}$ on the normalized lateral correlation length L for various roughness exponents α at a fixed $\Delta = 0.01$. For a fixed roughness exponent α, as L increases, the electric field ratio $\langle E \rangle / E^{(0)}$ decreases, but remains larger than 1. At very large L, the surface essentially becomes very smooth, and the roughness has no effect on the electric field. For a fixed L, as α decreases, the electric field ratio increases. For $L \ll 1$ and $\alpha = 0.3$, the electric field $\langle E \rangle$ can increase to about 15% of $E^{(0)}$. This may not seem so significant. Notice that the rms roughness w is only 1% of the thickness h_0 for this case. The change of electric field will be more significant for ultrathin dielectric films, where Δ is much larger than 0.01 for the same value of w.

It is worthwhile to point out that any complex dependence of the electrostatic potential and the electric field on the roughness parameters arises from α and ξ, and not from w. Because both the additional electric potential and electric field depend on the rms roughness amplitude w^2 through their relationships with the roughness spectrum simply as

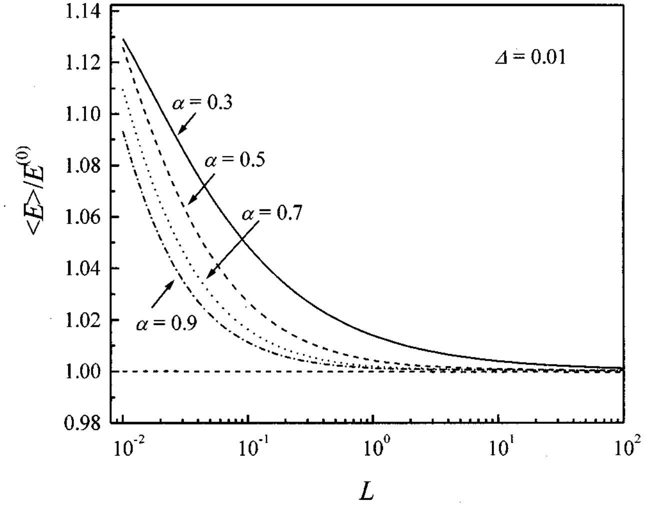

FIG. 3. Semilog plot of the ratio of electrostatic fields $\langle E \rangle / E^{(0)}$ as a function of the normalized lateral correlation length L ($= \xi/h_0$) for $\Delta = 0.01$, and α=0.3, 0.5, 0.7, and 0.9. Here $\Delta = w/h_0$.

$\langle |\tilde{h}(\mathbf{k})|^2 \rangle \sim w^2$. However, the roughness spectrum has a more complicated dependence on α and ξ; see Eq. (25).

V. ROUGHNESS EFFECTS ON CAPACITANCE WITH ONE ROUGH ELECTRODE

The surface charge density σ on a rough capacitor plate is given by $\sigma = \varepsilon \mathbf{E} \cdot \hat{\mathbf{n}}$ with $\hat{\mathbf{n}} = (\nabla h - \hat{\mathbf{e}}_3)/[1 + (\nabla h)^2]^{1/2}$ being the unit vector normal to a rough surface plate at $z = h_0 + h(\boldsymbol{\rho})$. Within the second-order perturbation expansion and an ensemble average over possible roughness configurations, the average capacitance $\langle C \rangle = \langle Q \rangle / V = \int \langle \sigma \rangle ds / V$ is given by

$$\langle C \rangle = \frac{A\varepsilon}{h_0} \left\{ 1 + \frac{1}{A} \int [\langle h \nabla^2 h \rangle + \langle (\nabla h)^2 \rangle] d\boldsymbol{\rho} + \frac{2\pi}{Ah_0} \int_{0<k<k_c} \frac{\cosh(kh_0)}{\sinh(kh_0)} k \langle |\tilde{h}(\mathbf{k})|^2 \rangle d\mathbf{k} \right\} \quad (32a)$$

Substituting the Fourier transforms

$$\int \langle (\nabla h)^2 \rangle d\boldsymbol{\rho} = \int \langle h \nabla^2 h \rangle d\boldsymbol{\rho} = \int_{0<k<k_c} k^2 \langle |\tilde{h}(\mathbf{k})|^2 \rangle d\mathbf{k}, \quad (32b)$$

into Eq. (32a) we obtain the expression

$$\langle C \rangle = \frac{A\varepsilon}{h_0} \left\{ 1 + \frac{2}{A} \int_{0<k<k_c} k^2 \langle |\tilde{h}(\mathbf{k})|^2 \rangle d\mathbf{k} + \frac{2\pi}{Ah_0} \int_{0<k<k_c} \frac{\cosh(kh_0)}{\sinh(kh_0)} k \langle |\tilde{h}(\mathbf{k})|^2 \rangle d\mathbf{k} \right\}. \quad (33)$$

To calculate morphology effects on $\langle C \rangle$ using Eq. (33), one needs the knowledge of a roughness spectrum. The excess capacitance due to surface roughness depends on the rms roughness amplitude w as $\langle C \rangle - C_0 \sim w^2$ because $\langle |\tilde{h}(\mathbf{k})|^2 \rangle \sim w^2$.

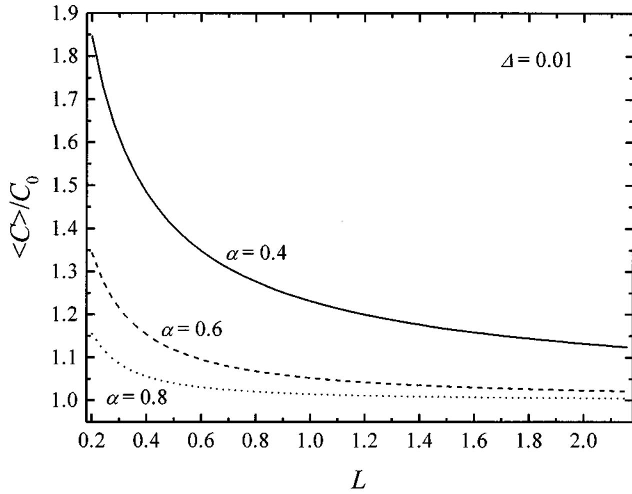

FIG. 4. Capacitance ratio $\langle C\rangle/C_0$ as a function of the normalized lateral correlation length $L(=\xi/h_0)$ for $\Delta=0.01$, and $\alpha=0.4$, 0.6, and 0.8. Here $\Delta=w/h_0$.

Figure 4 shows the calculated capacitance ratio $\langle C\rangle/C_0$ as a function of the normalized lateral correlation length L for various roughness exponents α. As the roughness exponent decreases (the rougher surface is at short wavelengths or $<\xi$) the roughness contributions drastically increase the capacitance by more than 30% for small roughness exponents $\alpha<0.5$ and a moderate roughness parameter ratio $w/\xi\sim 0.01$ close to the weak roughness limit (see Fig. 2). In fact, as the roughness exponent α decreases or the ratio w/ξ increases, the area of a rough capacitor plate increases. This leads effectively to a larger charge storage. Therefore, nanoscale surface roughness can drastically increase capacitance characteristics, altering microelectronic device operations and characteristics.

VI. ROUGHNESS EFFECTS ON LEAKAGE CURRENTS IN A CAPACITOR WITH ONE ROUGH ELECTRODE

Since the surface roughness can alter the average electrostatic field, it can also alter the leakage current of an insulating film. Independent of the mechanism that causes the leakage current, the leakage current density typically has an exponential relationship with the electric field. Therefore, the higher the field, the higher the leakage current density. For a rough electrode, due to the fluctuation of the surface height, the local electric field will vary from place to place, as we have derived in Eq. (23). At the peak of a rough surface, the electric field is larger than the valley, and we expect the leakage current density at the peak to be higher than that at the valley. If the leakage current density was only proportional to the electric field, then the average leakage current would show very little effect due to surface roughness. However, as the leakage current density changes exponentially with the electric field, the leakage current at the peak will gain more than the loss in the valley. Therefore, the net effect of surface roughness is to increase the leakage current density, even though other conditions are kept the same. In the following we take two conduction mechanisms, Schottky emission and the Poole-Frenkel effect, as examples to show how the surface roughness affects the leakage current density. Other conduction mechanism follows a similar method.

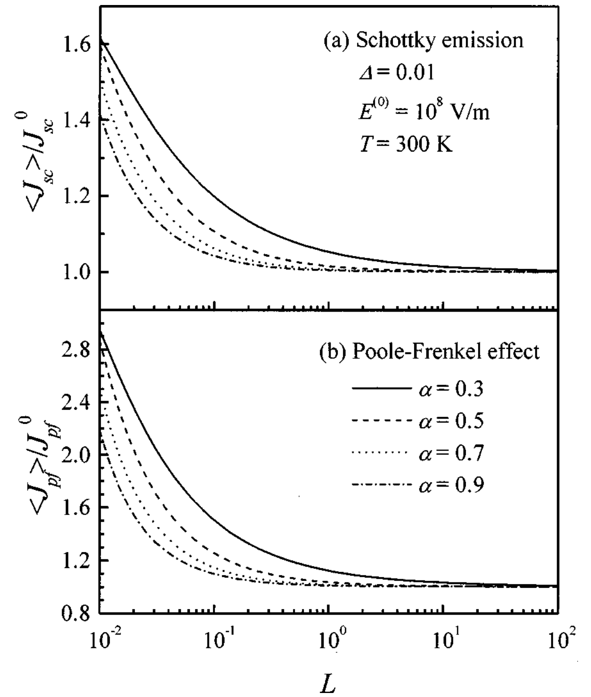

FIG. 5. Semilog plot of the leakage current density ratio for (a) Schottky emission and (b) the Poole-Frenkel effect as a function of the normalized lateral correlation length $L(=\xi/h_0)$ for $\Delta=0.01$, $E^{(0)}=10^8$ V/m, $T=300$ K, and roughness exponent $\alpha=0.3$, 0.5, 0.7, and 0.9. Here $\Delta=w/h_0$.

(a) Schottky emission: This type of conduction over the potential barrier of a metal/insulator interface is analogous to the thermionic emission, except that the applied electric field lowers the barrier height of the interface. The emission current density is given by[1,13]

$$J_{\rm sc}=A_s T^2 e^{-\Phi_B/KT} e^{\beta_s\sqrt{E}/KT}, \tag{34}$$

where $A_s(=120\ \mathrm{A/deg\,cm^2})$ being the Dushman-Richardson constant, $\beta_s=e^{3/2}/\sqrt{4\pi\varepsilon\varepsilon_0}$, ε_0 is the permittivity of the vacuum, and Φ_B is the Schottky potential barrier (depending on, e.g., metal work function, surface states, image forces, etc.) at the interface.[13]

(b) Poole-Frenkel effect: This effect is characterized by a mechanism similar to that of the Schottky effect, except that a field is applied to excite the thermal electrons from traps into the conduction band of an insulator.[1,13] The resulting current density has the form

$$J_{\rm pf}=\mu E e^{-\Phi_B/2KT} e^{2\beta_s\sqrt{E}/KT}, \tag{35}$$

where μ is the conductivity, and the barrier lowered by an applied field is twice that observed in Schottky emission. This is due to the immobility of positive charges associated with the traps.

In both cases, the main roughness contribution to a leakage current arises from the exponential dependence of the current, where the z component of the electric field (altered by roughness) yields the dominant effect. Thus, by making an expansion of the electric field E in Eqs. (34) and (35), we obtain the final leakage current formulas that incorporate roughness effects to the second-order perturbation theory:

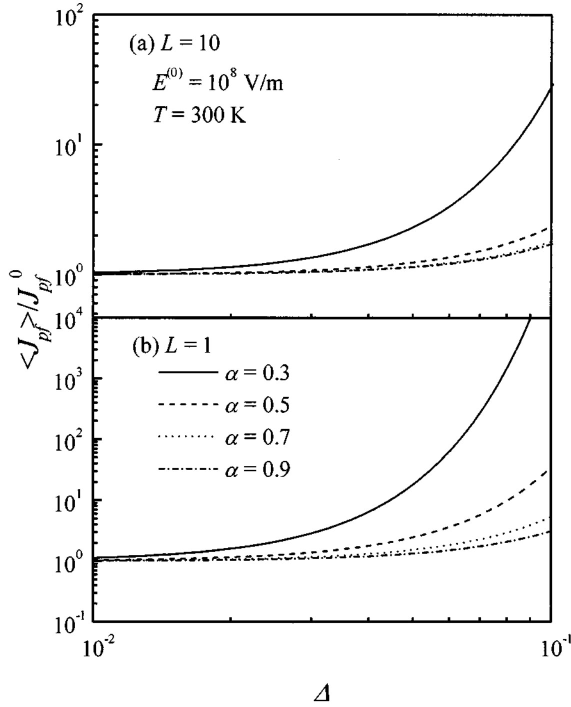

FIG. 6. The leakage current density ratio $\langle J_{\mathrm{pf}}\rangle/J_{\mathrm{pf}}^0$ for the Poole-Frenkel effect as a function of the normalized rms roughness Δ for (a) $L=10$ and (b) $L=1$ on a log-log scale at $E^{(0)}=10^8$ V/m, $T=300$ K, and roughness exponent $\alpha=0.3$, 0.5, 0.7, and 0.9. Here $L=\xi/h_0$ and $\Delta=w/h_0$.

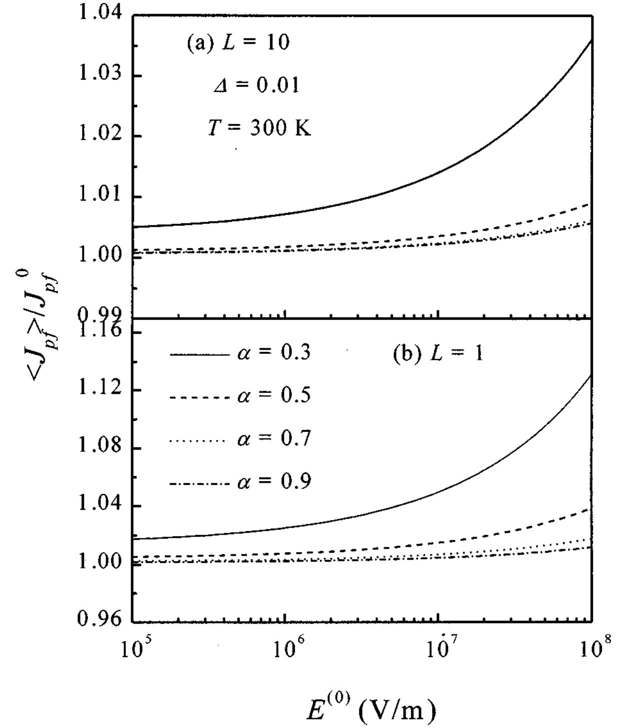

FIG. 7. Semilog plot of the leakage current density ratio $\langle J_{\mathrm{pf}}\rangle/J_{\mathrm{pf}}^0$ for the Poole-Frenkel effect as a function of the apparent field strength $E^{(0)}$ for (a) $L=10$ and (b) $L=1$ at $\Delta=0.01$, $T=300$ K, and roughness exponent $\alpha=0.3$, 0.5, 0.7, and 0.9. Here $L=\xi/h_0$ and $\Delta=w/h_0$.

For Schottky emission assuming $\langle E^{(2)}\rangle/E^{(0)}\ll 1$, we obtain

$$\frac{\langle J_{\mathrm{sc}}\rangle}{J_{\mathrm{sc}}}=\exp\left(\frac{\beta_s\sqrt{E^{(0)}}}{2kT}\frac{\langle E^{(2)}\rangle}{E^{(0)}}\right), \tag{36}$$

where $J_{\mathrm{sc}}^0=A_sT^2e^{-\Phi_B/KT}e^{-\beta_s\sqrt{E^{(0)}}/KT}$ is the unperturbed leakage current density for a smooth metal/insulator interface, and the ratio $\langle E^{(2)}\rangle/E^{(0)}$ can be obtained from Eq. (30).

For the Poole-Frenkel effect we obtain

$$\frac{\langle J_{\mathrm{pf}}\rangle}{J_{\mathrm{pf}}^0}=\left(1+\frac{\langle E^{(2)}\rangle}{E^{(0)}}\right)\exp\left(\frac{\beta_s\sqrt{E^{(0)}}}{kT}\frac{\langle E^{(2)}\rangle}{E^{(0)}}\right), \tag{37}$$

with $J_{\mathrm{pf}}^0=\mu E^{(0)}e^{-\Phi_B/KT}e^{-2\beta_s\sqrt{E^{(0)}}/KT}$ being the unperturbed leakage current density for a smooth metal/insulator interface.

Equations (36) and Eq. (37) are very similar. From the discussion of the electric field in Sec. IV, we learned that $\langle E^{(2)}\rangle\propto w^2$. Therefore, we expect that the leakage current density increases exponentially with w^2. Also, since $\langle E^{(2)}\rangle$ decreases monotonically with increasing normalized lateral correlation length L and increasing roughness exponent α, we would expect a similar behavior in the leakage current density. Figure 5 shows the dependence of the Schottky and Poole-Frenkel leakage current densities on the normalized lateral correlation length L for various values of α at $\Delta=0.01$. In both cases our calculations were performed for an insulating film with relatively low permittivity $\varepsilon=3.9$ (which corresponds to SiO_2), and a field strength $E^{(0)}=10^8$ V/m at room temperature $T=300$ K. We see that Fig. 5 has a similar behavior to that of Fig. 3, as expected. The only difference between Schottky emission and the Poole-Frenkel effect is that for the same rough surface the leakage current density in Poole-Frenkel effect is higher than that in Schottky emission. In Fig. 6 we plot the leakage density ratio $\langle J_{\mathrm{pf}}\rangle/J_{\mathrm{pf}}^0$ as a function of the normalized interface width Δ for (a) $L=10$ and (b) $L=1$ at different roughness exponent α values. The field strength $E^{(0)}=10^8$ V/m. Clearly the leakage current increases drastically with the increases of the normalized interface width Δ. For a relative smooth surface $L=10$, the leakage current density can be almost 30 times greater at $\Delta>0.1$ and $\alpha=0.3$. However, as L decreases, the effect of interface width w becomes even more significant, as shown in Fig. 6(b). It is also interesting to note that even for the same rough surface, the change of the applied field strength $E^{(0)}$ will also change the degree of the roughness effect. Figure 7 shows the leakage current density ratio as a function of the applied field strength $E^{(0)}$ for (a) $L=10$ and (b) $L=1$ at $\Delta=0.01$. The ratio $\langle J_{\mathrm{pf}}\rangle/J_{\mathrm{pf}}^0$ increases as $E^{(0)}$ increases, but the effect is not so significant under the condition $\Delta=0.01$ that we considered in Fig. 7.

VII. DISCUSSIONS AND CONCLUSIONS

The above treatments for both the capacitance and the leakage current are based on a mean-field point of view. There are still some open questions. For the capacitance, in practice the size of the electrode cannot be infinite. In this case one needs to consider the edge effect of the capacitance. In general the edge effect will contribute a geometric factor, which tends to increase the capacitance.[16] If the size of the

electrode is much larger than the lateral correlation of the rough electrode, we would expect a similar behavior of the capacitance as in the infinite electrode case. However, if the electrode size is smaller than the lateral correlation length of the rough electrode, since only limited spatial frequency from the roughness will contribute to the capacitance, then the total contribution from the rough surface will decrease. This is only a simple extrapolation from our above discussion; detailed behavior can be obtained by solving the finite-size capacitor bounded by one rough electrode.[20]

Another issue is the critical breakdown field strength E_c under the presence of surface roughness. In Sec. IV we have shown that surface roughness will increase the field $E^{(0)}$ to the effective electric field by $E^{(0)}+\langle E^{(2)}\rangle$ inside the insulating film. If we assume the critical field for an insulating film is fixed, then the presence of surface roughness will reduce the breakdown field by a value of $\langle E^{(2)}\rangle$. This intuitive discussion may work fine for a thermal breakdown, since in order to induce the breakdown, the heat generated by the electric field cannot be localized. However, for a pure electrical breakdown, a localized breakdown may happen first, especially at the peak of a rough surface. This localized breakdown requires only a much smaller electric field, $E^{(0)}$, and opens conducting channels from the upper electrode to the lower electrode. As the field increases, those channels become wider and wider. Those opened channels will definitely enhance the electric fields in the vicinities of the peaks, and therefore at a certain field strength they cause a global breakdown. A detailed investigation of such a behavior is still not available.

We have to point out that in actual experimental situations the conduction mechanism might have a more complex behavior. It has been observed in crystalline and amorphous Ta_2O_5 films (deposited on SiO_2/n-Si substrates) with a relatively high dielectric constant $\varepsilon_r\approx 31$, under a moderate field $(10^7-3.5\times 10^7$ V/m), that the conduction processes are electrode limited (Schottky emission), while under higher fields $(>3.5\times 10^7$ V/m) conduction processes are bulk limited (Poole-Frenkel emission).[21] As shown in Fig. 5, one would expect that the roughness will have different impact on the leakage current.

We investigated roughness effects on electrical properties in a parallel-plate capacitor with one smooth electrode and the other roughened at nanometer length scales. Qualitatively similar results would be expected for capacitors with double rough plates as well as for other geometries. We found that the roughness can cause a stronger effective field $E^{(0)}+\langle E^{(2)}\rangle$ than the field $E^{(0)}$. The excessive field $\langle E^{(2)}\rangle$ caused by surface roughness is proportional to w^2, and has a complicated relation with ξ and α. In general, $\langle E^{(2)}\rangle$ decreases when either ξ or α increases. The effect of a rough surface also increases the capacitance, and it has a similar effect on the electric field. In addition, we examined qualitatively how weak roughness perturbations can affect the leakage current in the capacitor for two distinct cases. It was shown that for Schottky and Poole-Frenkel emissions, the roughness effects within the weak roughness limit can give a significant contribution to the leakage current for a moderate field strength even at room temperature $T\sim 300$ K. For these types of leakage current, an increase of roughness at any wavelength (α decreasing and ratio w/ξ increasing) is shown to increase the leakage current. Results from many experiments have trends which agree qualitatively with our predictions.[8–12] Further experimental studies on thin-film capacitors with known roughness would be required to establish a quantitative connection with our theoretical predictions.

ACKNOWLEDGMENTS

This work was supported in part by NSF, SRC Center for Advanced Interconnect Science and Technology, and MARCO Focus Center Research Program. G.P. would like to acknowledge the support from the Netherlands Institute for Metals Research (NIMR). We thank Professor E. Rymazaeski for valuable discussions.

[1] S. M. Sze, *Semiconductor Devices: Physics and Technology* (Wiley, New York, 1985).

[2] K. A. McKinley and N. P. Sandler, Thin Solid Films **290**, 440 (1996).

[3] H. Shinriki, Y. Nishioka, Y. Ohij, and K. Mukai, Tech. Dig. Int. Electron Devices Meet. **32**, 684 (1986); H. Saitoh, T. Mori, and H. Tamura, *ibid.* **32**, 680 (1986).

[4] J. H. Oh, Y. H. Lee, B. K. Ju, D. K. Shin, C. Y. Park, and M. H. Oh, J. Appl. Phys. **82**, 6203 (1997).

[5] M. C. Lopes, S. G. dos Santos, and C. M. Hasenack, J. Electrochem. Soc. **143**, 1021 (1996).

[6] T. S. Rahman and A. A. Maradudin, Phys. Rev. B **21**, 504 (1980); G. Palasantzas, J. Appl. Phys. **82**, 351 (1997); F. J. Ohkawa and Y. Uemura, Prog. Theor. Phys. Suppl. **57**, 164 (1975); T. Ando, J. Phys. Soc. Jpn. **39**, 411 (1975).

[7] T. Ando, A. B. Fowler, and F. Stern, Rev. Mod. Phys. **54**, 437 (1982); A. Hartstein, T. H. Ning, and A. B. Fowler, Surf. Sci. **58**, 178 (1976); T. Ando, J. Phys. Soc. Jpn. **51**, 3900 (1982); G. Fishman, and D. Calecki, Phys. Rev. Lett. **62**, 1302 (1989); Phys. Rev. B **43**, 11 581 (1991); H. Sakaki, T. Noda, K. Hirakawa, M. Tanaka, and T. Matsusue, Appl. Phys. Lett. **51**, 1934 (1987); G. Palasantzas and J. Barnas, Phys. Rev. B **56**, 7726 (1997); Phys. Status Solidi B **209**, 319 (1998); J. Barnas and G. Palasantzas, J. Appl. Phys. **82**, 3950 (1997).

[8] A. Chin, B. C. Lin, W. J. Chen, Y. B. Lin, and C. Tsai, IEEE Electron Device Lett. **19**, 426 (1998).

[9] K. Okada (unpublished).

[10] Ho Jin Cho and Hyeong Joon Kim, J. Electrochem. Soc. **145**, 3884 (1998).

[11] Tingkai Li, P. Zawadzki, R. A. Stall, Yongfei Zhu, and S. B. Desu, in *Structure and Evolution of Surfaces*, edited by R. C. Cammarata, E. H. Chason, T. L. Einstein, and E. D. Williams, MRS Symposium Proceedings No. 440 (Materials Research Society, Pittsburgh, 1997), p. 315.

[12] Ke Chen, M. Nielsen, S. Soss, E. J. Rymaszewski, T.-M. Lu, and C. T. Wan, IEEE Trans. Compon., Packag. Manuf. Technol., Part B **20**, 117 (1997).

[13] D. R. Lamb, *Electrical Conduction Mechanisms in Thin Insulat-*

ing Films (Spottiswoode, London, 1967); J. J. O'Dwyer, *The Theory of Electrical Conduction and Breakdown in Solid Dielectrics* (Oxford University Press, Oxford, 1973); K. D. Leaver and B. N. Chapman, *Thin Films* (Wykeham, London, 1971).

[14] P. Meakin, Phys. Rep. **235**, 1991 (1993); J. Krim and G. Palasantzas, Int. J. Mod. Phys. B **9**, 599 (1995); F. Family and T. Viscek, *Dynamics of Fractal Surfaces* (World Scientific, Singapore, 1991); A.-L. Barabasi and H. E. Stanley, *Fractal Concepts in Surface Growth* (Cambridge University Press, New York, 1995); H.-N. Yang, G.-C. Wang, and T.-M. Lu, *Diffraction from Rough Surfaces and Dynamic Growth Fronts* (World Scientific, Singapore, 1993).

[15] S. K. Sinha, E. B. Sirota, S. Garoff, and H. B. Stanley, Phys. Rev. B **38**, 2297 (1988).

[16] G. Palasantzas, Phys. Rev. B **48**, 14 472 (1993); **49**, 5785(E) (1994). Besides the simplicity of $\langle|\tilde{h}(\mathbf{k})|^2\rangle$, its Fourier transform yields the analytically solvable correlation function $C(r) = [w^2/a\Gamma(1+\alpha)](r/2a^{1/2}\xi)^{\alpha}K_H(r/2a^{1/2}\xi)$, with $K_\nu(x)$ being the second kind of Bessel function of order ν.

[17] H.-N. Yang and T.-M. Lu, Phys. Rev. B **51**, 2479 (1995); Y.-P. Zhao, G.-C. Wang, and T.-M. Lu, Phys. Rev. B **55**, 13 938 (1997); G. Palasantzas and J. Krim, *ibid.* **48**, 2873 (1993); G. Palasantzas, Phys. Rev. E **49**, 1740 (1994).

[18] G. Palasantzas, Phys. Rev. E **56**, 1254 (1997) [in terms of Eq. (3.2) the rms local surface slope ρ is given in an analytic form]; J. H. Jeffries, J.-K. Zuo, and M. M. Craig, Phys. Rev. Lett. **76**, 4931 (1996); J. G. Amar, P. M. Lam, and F. Family, Phys. Rev. E **47**, 3242 (1993); T.-M. Lu, H.-N. Yang, and G.-C. Wang, in *Fractal Aspects of Materials*, edited by F. Family, P. Meakin, B. Sapoval, and R. Wool, MRS Symposium Proceedings No. 367 (Materials Research Society, Pittsburgh, 1995), p. 283.

[19] G. Palasantzas and J. Krim, Phys. Rev. Lett. **73**, 3564 (1994).

[20] G. T. Carlson and B. L. Illman, Am. J. Phys. **62**, 1099 (1994).

[21] E. Ezhilvalavan and T.-Y. Tseug, J. Appl. Phys. **83**, 4797 (1998); F.-C. Chiu, J.-J. Wang, J. Y.-M. Lee, and S.-C. Wu, *ibid.* **81**, 6911 (1997); J. G. Simmons, Phys. Rev. B **166**, 912 (1968).